ISSN 1560-3547, Regular and Chaotic Dynamics, 2018, Vol. 23, No. 4, pp. 458–470. © Pleiades Publishing, Ltd., 2018.

Hyperbolic Chaos in Systems Based on FitzHugh – Nagumo Model Neurons

Sergey P. Kuznetsov[1, 2*] and Yuliya V. Sedova[1]**

[1] *Kotel'nikov's Institute of Radio-Engineering and Electronics of RAS, Saratov Branch, ul. Zelenaya 38, Saratov, 410019 Russia*

[2] *Udmurt State University, ul. Universitetskay 1, Izhevsk, 426034 Russia*

Received May 06, 2018; accepted June 04, 2018

Abstract—In the present paper we consider and study numerically two systems based on model FitzHugh – Nagumo neurons, where in the presence of periodic modulation of parameters it is possible to implement chaotic dynamics on the attractor in the form of a Smale – Williams solenoid in the stroboscopic Poincaré map. In particular, hyperbolic chaos characterized by structural stability occurs in a single neuron supplemented by a time-delay feedback loop with a quadratic nonlinear element.

MSC2010 numbers: 37D05, 37D20, 37D45, 37M25, 82C32, 92B20

DOI: 10.1134/S1560354718040068

Keywords: hyperbolic chaos, Smale–Williams solenoid, FitzHugh – Nagumo neuron, time-delay system

1. INTRODUCTION

The FitzHugh – Nagumo model [1, 2] provides one of the examples of the interdisciplinary approach inherent in the theory of oscillations and waves [3–6], when similar equations are used to describe objects of different physical nature, so that the understanding of phenomena taking place in one field of science deepens and enriches the understanding of the behavior of objects in another field. With respect to the FitzHugh – Nagumo model, we are talking about equations providing a phenomenological description of a neuron which are also applicable to an electronic circuit known as the Bonhoeffer – van der Pol oscillator.

Construction of different variants of composite systems based on elements described by the FitzHugh – Nagumo equations, including systems with time-delay feedback, is of interest for many reasons. Firstly, this is a way for model description of real phenomena that can occur in natural neural systems. Secondly, analog simulation of complex neural systems by means of electronic circuits is possible, which essentially corresponds to the initial premises of FitzHugh's paper [1] appealing to the analogy with the Bonhoeffer – van der Pol oscillator, and to Nagumo's work [2] based on reproduction of phenomena accompanying the propagation of impulses in the axon by means of a transmission line on tunnel diodes. Thirdly, studies of coupled systems and time-delay systems based on model neurons can help to reveal possibilities of phenomena that are known in the modern theory of dynamical systems at the level of abstract mathematical concepts, but still await detection and application in real-world systems. This direction of research can open up prospects of designing new technical devices that reproduce some properties of natural neural systems, as well as devices with new functionalities.

In this paper we will discuss uniformly hyperbolic attractors, the objects in state space of dynamical systems introduced in mathematical theory in the 1960s–1970s [7–9]. The specific nature of these attractors is that they are composed exclusively of saddle trajectories, in which the contracting and expanding invariant subspaces can be distinguished in the tangent space of vectors of infinitesimal perturbations. The first invariant subspace is formed by vectors, the norms of which decrease exponentially in direct time, and the second is formed by vectors whose norms decrease

* E-mail: spkuz@yandex.ru

** E-mail: sedovayv@yandex.ru

exponentially in reverse time. Thus, an arbitrary vector of small perturbation is represented by a linear combination of vectors belonging to both of these subspaces. The sets of representing points approaching a given trajectory in direct or reverse time correspond, respectively, to the stable and unstable manifolds of this trajectory. For a hyperbolic attractor these manifolds can intersect, but must not have tangencies.

The fundamental mathematical fact is that the hyperbolic chaos has a property of roughness, or structural stability. After the studies of Andronov and Pontrjagin [3, 10], in the theory of oscillations it is customary to postulate that of the primary theoretical and practical interest are precisely the rough systems that demonstrate motions, which do not change qualitatively with a little variation of parameters and functions in the evolution equations. Within the framework of chaos theory, this property seems extremely important for natural systems and technical applications, since it would ensure insensitivity of the chaos characteristics to inaccuracy in setting parameters, manufacturing errors, noise and disturbances. However, as the theory of dynamical systems and its applications evolved, it became clear that numerous examples of chaotic dynamics, which occur in various fields of science and technology, do not satisfy this property. The lack of structural stability leads to observable phenomena of destruction of chaos accompanied by the appearance of "windows of regularity" under small variations in the system parameters; this is associated with the concept of quasi-attractor [9]. It was not until most recently that some physical examples of systems with structurally stable hyperbolic chaos were proposed and implemented [11, 12].

Recently, it has been shown that chaotic dynamics associated with hyperbolic attractors such as the Smale – Williams solenoid in the Poincaré map can be designed on the basis of coupled FitzHugh – Nagumo elements alternately excited by external parameter modulation [13, 14]. In the present paper, we will also consider a system with hyperbolic chaos using a single FitzHugh – Nagumo neuron supplemented with time-delay feedback. (Other examples of nonlinear systems, where time-delay feedback was used to implement hyperbolic chaos, were discussed in [15–20].)

In Section 2, we recall the model and results of Ref. [13], drawing on the analysis of the parameter space structure by means of a chart of regimes composed with the help of Lyapunov exponents computations. Section 3 introduces a system with modulation of the control parameters based on a single model FitzHugh – Nagumo neuron with a time-delay feedback loop with quadratic nonlinearity. It is shown that the dynamics of such a system is in many respects similar to that in the model [13]. Particularly, in a wide range of parameters, the stroboscopic map possesses a chaotic hyperbolic attractor in the form of a Smale – Williams solenoid. Section 4 presents results of a numerical test of the hyperbolic nature of attractors in the system with time-delay by numerical calculation and analysis of statistics of the angles of intersections of the expanding and contracting manifolds of trajectories at the attractor. In the Conclusion we summarize results of the study and briefly discuss some prospects for research on systems based on model neurons using the proposed techniques and analog simulation by means of electronic circuits.

2. SMALE – WILLIAMS ATTRACTOR IN A SYSTEM OF TWO COUPLED ALTERNATELY EXCITED FITZHUGH – NAGUMO NEURONS

Equations of an individual FitzHugh – Nagumo subsystem have the form

$$\begin{aligned} \dot{x} &= cx - x^3/3 - y, \\ \dot{y} &= ax - by + I, \end{aligned} \tag{2.1}$$

where x and y are the dynamical variables that have the meaning of the membrane potential and the slow recovery variable, respectively, a, b and c are parameters considered as constant in the original model, and I is the external current across the membrane.

In [13], a model was introduced composed of a symmetric pair of FitzHugh – Nagumo elements

$$\begin{aligned} \dot{x} &= c_0 x - \frac{1}{3}x^3 - y, \\ \dot{y} &= (a_0 + a_1 \sin \Omega t)x - (b_0 + b_1 \cos \Omega t)y + \varepsilon \dot{u}^2, \\ \dot{u} &= c_0 u - \frac{1}{3}u^3 - v, \\ \dot{v} &= (a_0 - a_1 \sin \Omega t)u - (b_0 - b_1 \cos \Omega t)v + \varepsilon \dot{x}^2, \end{aligned} \tag{2.2}$$

where the variables x, y relate to the first subsystem, and u, v to the second, and the parameters of the subsystems are periodically modulated in such a way that it provides their alternate activity; the coupling is selected through quadratic nonlinearity to ensure the transfer of excitation from one neuron to another accompanied by doubling of the phase of oscillations.

Equations (2.2) have an obvious symmetry with respect to the substitution

$$x \to u,\ y \to v,\ u \to x,\ v \to y,\ t \to t + \pi/\Omega. \tag{2.3}$$

The functioning of the system proceeds as follows. Let the oscillations of the first subsystem in the active stage (the first half-period) have a certain phase φ, that is, $x \sim \cos(\omega_0 t + \varphi)$. In half a period, the second oscillator becomes active. The stimulus for its initial excitation is the second harmonic of the signal produced by the first oscillator, $\dot{x}^2 \sim \sin^2(\omega_0 t + \varphi) = \frac{1}{2} - \frac{1}{2}\cos(2\omega_0 t + 2\varphi)$, so the resulting oscillations inherit the phase 2φ+const. In the absence of resonance for small-amplitude oscillations [22] the transfer of the excitation from the first oscillator to the second one at the doubled frequency $2\omega_0$ is facilitated by the fact that the nonlinearity parameter is chosen negative, $\beta < 0$. Because of the "soft spring" principle, the oscillation frequency of the first oscillator is less than ω_0, and the excitation at the second harmonic with doubled phase of the oscillations is still transmitted. When the active stage of the second oscillator comes to an end, it transmits the excitation to the first one, which just becomes active exactly in the same manner, and so on. Thus, one step of the excitation exchange is accompanied by doubling of the phase variable defined modulo 2π, in accordance with the expanding circle map (Bernoulli map). As the phase volume is compressed in other directions, this corresponds to the presence of an attractor in the form of a Smale – Williams solenoid in the phase space.

Figure 1 shows waveforms for the variables x and u of the system (2.2) with a set of parameters corresponding to the mode of operation described above. The waveforms have typical form inherent in many neuron models called "bursts", sequences of rapid oscillations of the membrane potential variable, alternating with regions of smooth decay/recovery of the activity. In our case, the appearance of successive bursts is due to the periodic modulation of the parameters of the subsystems, and here the phases of the oscillations ("spikes") vary from one to another burst according to the Bernoulli map, i. e., chaotically.

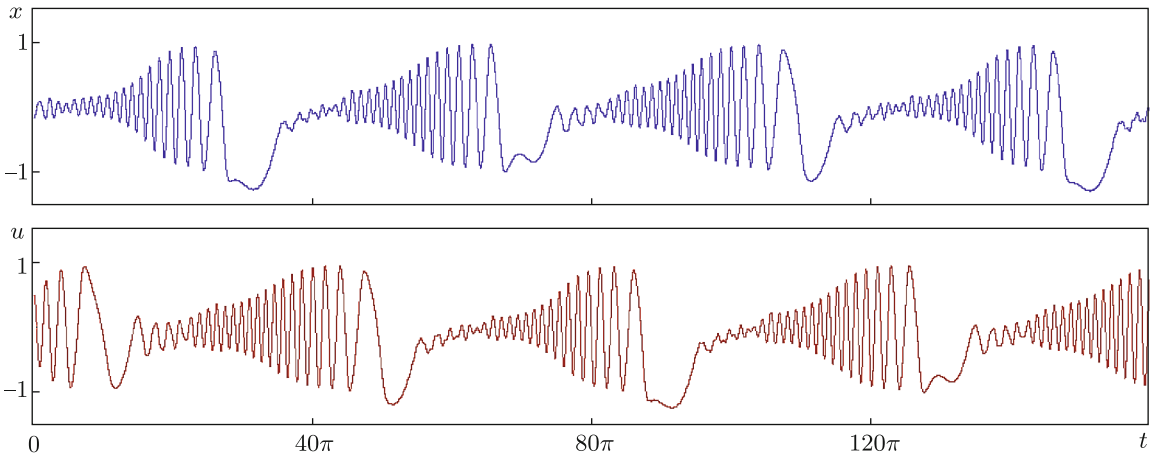

Fig. 1. Waveforms of dynamical variables $x(t)$ and $u(t)$ on four periods of modulation of parameters for the system (2.2). Values of the parameters: $a_0 = a_1 = 1.5$, $b_0 = b_1 = 0.1$, $c_0 = 0.2$, $\varepsilon = 0.3$, $\Omega = 0.05$.

Since the system examined is nonautonomous, with periodic variation of the coefficients, we can describe the dynamics in discrete time by means of the Poincaré stroboscopic map. In our case, taking into account the symmetry of the system, it is appropriate to use the map in a half-period of modulation, determining the state vector at the moments of time $t_n = \pi n/\Omega = nT$ as

$$\mathbf{X}_n = (x_1, x_2, x_3, x_4)_n = \begin{cases} \big(x(nT),\ y(nT),\ u(nT),\ v(nT)\big), & \text{if } n \text{ is odd}, \\ \big(u(nT),\ v(nT),\ x(nT),\ y(nT)\big), & \text{if } n \text{ is even}. \end{cases} \tag{2.4}$$

The four-dimensional Poincaré map may be written formally as

$$\mathbf{X}_{n+1} = \mathbf{F}_{T/2}(\mathbf{X}_n). \tag{2.5}$$

It can be realized as a computer program that integrates Eqs. (2.2) on a half-period of the modulation.

Figure 2a shows a phase portrait of the attractor of the map (2.5), which is a two-dimensional projection of the Smale – Williams solenoid. The inset is a magnified fragment resolving the transverse fractal structure inherent in the solenoid. The fact that each step of evolution in discrete time is accompanied by doubling of the angular coordinate on the solenoid filaments is illustrated by the diagram in Fig. 2b. Here, along the coordinate axes, the values of the angular variable are plotted at the nth and $(n+1)$st moments of discrete time as obtained from the results of numerical integration of Eqs. (2.2) on successive modulation periods with the formula $\varphi_n = \arg[(x_1 + ix_2)]_n$.

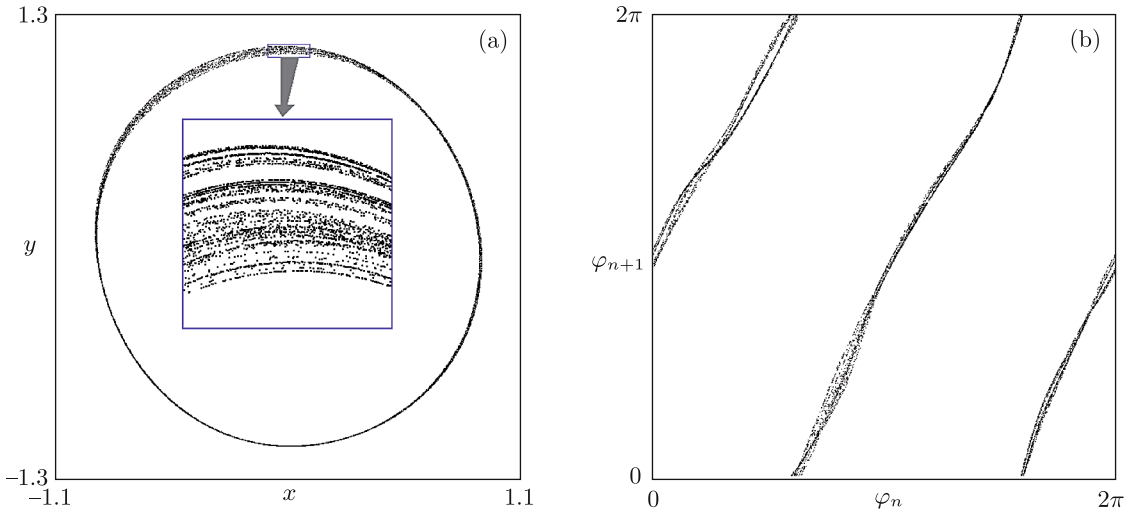

Fig. 2. Two-dimensional projection of the Smale – Williams attractor for the Poincaré map (a), where the transverse structure of the solenoid is shown with magnification by the inset, and the diagram of the phases of the spike oscillations corresponding to successive bursts, which illustrates the doubling of the angular variable in a half-period of the modulation (b). Parameters: $a_0 = a_1 = 1.5$, $b_0 = b_1 = 0.1$, $c_0 = 0.2$, $\varepsilon = 0.3$, $\Omega = 0.05$.

Four Lyapunov exponents of the attractor found for the map (2.5) from the results of computations using the numerical solution of (2.2) and the corresponding set of variational equations, with Gram – Schmidt orthogonalization of the perturbation vectors, are

$$\Lambda = \{0.670,\ -1.054,\ -4.13,\ -18.16\}. \tag{2.6}$$

The presence of a positive exponent indicates a chaotic nature of the dynamics. Its proximity to $\ln 2$ is due to the fact that the angular variable undergoes doubling on successive iterations. The other exponents are negative and are responsible for formation of the transverse fractal structure of the solenoid. To estimate the dimension of the attractor, we can use the Kaplan – Yorke formula [23–25]

$$D = m + |\Lambda_{m+1}|^{-1} \sum_{i=1}^{m} \Lambda_i, \tag{2.7}$$

where in the general case m is defined so that $S_m = \sum\limits_{i=1}^{m} \Lambda_i > 0$, but $S_{m+1} = \sum\limits_{i=1}^{m+1} \Lambda_i < 0$. In our situation it gives $D_{KY} = 1 + \Lambda_1/|\Lambda_2| \approx 1.64$.

Figure 3 shows a plot of Lyapunov exponents of the map (2.5) versus parameter c with other parameters constant. It should be noted that there is a wide range in which the exponent Λ_1 remains approximately constant and close to $\ln 2$. As can be seen, this region, where chaotic dynamics is

determined by the Smale – Williams attractor, is continuous; this observation testifies in favor of the structural stability of chaos. At the left and right edges we can see a distinct behavior of Λ_1 with dips in the graph, which correspond to the windows of periodicity in the region where chaos is nonhyperbolic. The range on the right side of the graph, where the Lyapunov exponent is zero (up to calculation accuracy), corresponds to quasi-periodic dynamics.

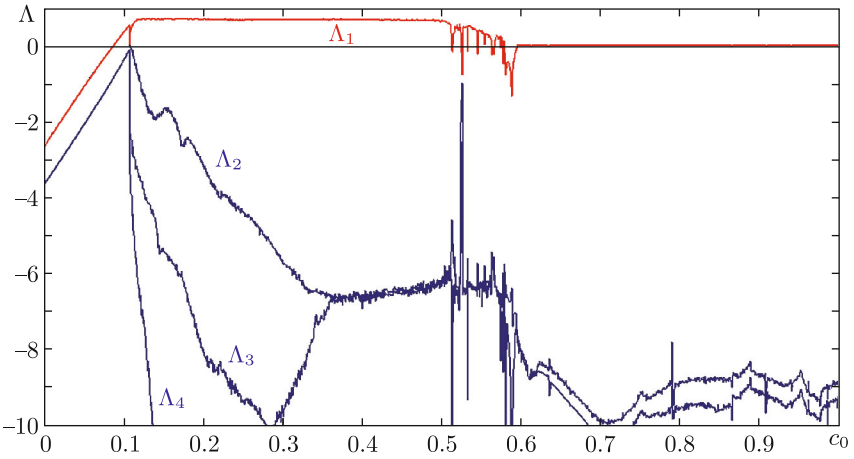

Fig. 3. Lyapunov exponents of the map (2.5) versus parameter c_0 with $\Omega = 0.05$, $\varepsilon = 0$, $a_0 = a_1 = 1.5$, $b_0 = b_1 = 0.1$.

Figure 4 shows a chart of regimes of the system (2.2) in the parameter plane. For its computation, the selected region was scanned with a small step in two coordinates. Each pixel is color-coded in accordance with the regime diagnosed at the respective point, which occurs as the equations are numerically integrated. If all the exponents are negative, then it corresponds to a regular periodic mode, namely, an attractive fixed point or a periodic cycle of the Poincaré map. The closeness of the largest exponent to zero indicates quasi-periodic dynamics, which in the phase space of the Poincaré map corresponds to an attractive closed invariant curve. The presence of a positive exponent indicates existence of chaotic attractor, which may be hyperbolic or nonhyperbolic.

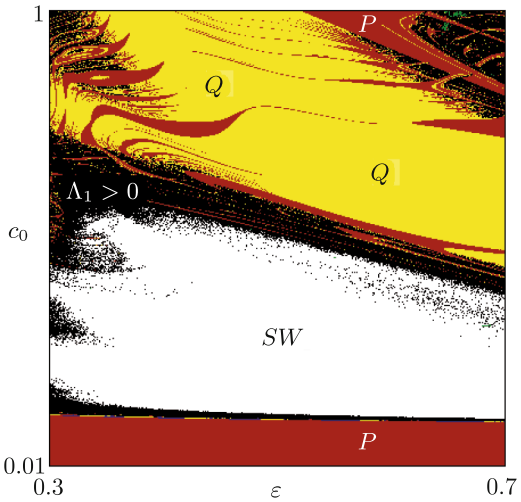

Fig. 4. Chart of regimes of the system (2.2) on the parameter plane (ε, c_0). Regions of different modes are marked with colors identified by analysis of the spectrum of Lyapunov exponents as explained in the text. The white region SW ($\Lambda_1 \approx \ln 2$) is roughly associated with the hyperbolic chaotic Smale – Williams attractor; the black region is nonhyperbolic chaos ($\Lambda_1 > 0$); the red region P corresponds to the periodic dynamics ($\Lambda_1 < 0$), and the yellow region Q, to quasi-periodic dynamics ($\Lambda_1 \approx 0$).

Plotting the chart, as a diagnostic tool for distinguishing the hyperbolic Smale – Williams attractor of the Poincaré map, we exploit the proximity of the positive Lyapunov exponent to the value $\ln 2$ corresponding to the Bernoulli map. Although this cannot be considered as an accurate quantitative criterion, control calculations confirm that with this method the hyperbolicity region is determined rather correctly: iteration plots for the angular variable at the points of the found area qualitatively correspond to Fig. 2b (a graph in the form of two branches close to straight lines with a slope coefficient of 2). Hyperbolic chaos, in accordance with its inherent property of structural stability, occupies a continuous area in the parameters plane, denoted as SW. The hyperbolic nature of chaos was also confirmed by computational verification of absence of tangencies of stable and unstable manifolds for trajectories on an attractor as described in [13, 14]. (In the present paper, a special section (Section 4) is devoted to this criterion, adapted for the time-delay system.)

The exit from the SW region by variation of parameters is associated with different scenarios of the destruction of hyperbolic chaos [26].

If we move to the left in the parameter plane, then, as we approach the boundary of hyperbolicity, on the iterative diagrams for the angular variable we can observe the appearance of inflection points (local places of zero slope). Accordingly, the distribution of the invariant measure along the filaments of the solenoid becomes nonsmooth, and singularities arise, which corresponds to violation of the uniform hyperbolicity.

As we approach the lower boundary of the region, we see an increase in the width of the toroidal domain containing the Smale – Williams solenoid, and then what happens can be described as "disappearance of the donut hole". The angular variable in this case is not defined everywhere, because of which on the iterative diagram exclusive points appear that do not fall on the pronounced branches, which correspond to the expanding circle map of Bernoulli. A similar scenario occurs when we pass through the upper boundary. After exit from the hyperbolicity domain, the topological nature of the map for the angular variable changes; instead of the Bernoulli map with two branches, a single-valued circle map is observed. Such a map generates either quasi-periodic dynamics or periodic behavior corresponding to the Arnold synchronization tongues [25, 27, 28]. The respective areas Q and P occupy a broad zone at the top part of the chart. In the upper right corner of the chart we can see a characteristic picture inherent in the classical circle map, where nonhyperbolic chaos takes place; the area contains periodicity in narrow bands and shrimp-like formations [29].

3. SMALE – WILLIAMS ATTRACTOR IN THE DYNAMICS OF A SINGLE NEURON WITH TIME-DELAY FEEDBACK

The idea of constructing a model with hyperbolic chaos on the basis of a single neuron with parameter modulation is to modify the system considered in the previous section replacing the partner system by transmission of excitation from one and the same oscillator by means of an additional time-delay feedback loop. Namely, let us consider time-delay equations of the following form:

$$\begin{aligned} \dot{x} &= c_0 x - \frac{1}{3}x^3 - y, \\ \dot{y} &= (a_0 - a_1 \sin \Omega t)x - (b_0 - b_1 \cos \Omega t)y + \varepsilon \dot{x}^2(t-\tau). \end{aligned} \tag{3.1}$$

The delay time τ may generally be regarded as an additional parameter, which can be varied to obtain different dynamical behaviors, but we will usually assume that it is equal to the half-period of modulation $\tau = \pi/\Omega$.

It is important to emphasize that systems with delay are characterized by an infinite dimension of the phase space [24, 30, 31]. In fact, in order to specify a state of the system (3.1) that allows uniquely determining the subsequent dynamics, it is necessary to set not only the values of x and y at an initial moment of time, but also to set the function $\dot{x}(t-\tau)$ on the previous time interval of duration τ.

For the system (3.1) we can determine the stroboscopic map for the period $T = 2\pi/\Omega$:

$$\mathbf{X}_{n+1} = \mathbf{F}_T(\mathbf{X}_n), \tag{3.2}$$

but, in contrast to the map (2.5), the vector $\mathbf{X}_n$ now must be interpreted as an element of an infinite-dimensional space that defines a system state at $t_n = nT$.

The principle of the system functioning is similar to that discussed in the previous section. Let oscillations in the active stage have a certain phase φ, that is, $x \sim \cos(\omega_0 t + \varphi)$, and let the generated signal be transmitted to the feedback channel. After the stage of oscillations damping and a new transition to the activity stage, the excitation of the oscillator is stimulated by the second harmonic of the signal passed through the feedback loop with quadratic transformation according to $\dot{x}^2(t-\tau) \sim -\frac{1}{2}\cos(2\omega_0 t + 2\varphi + \text{const}) + \ldots$, so that the oscillations get the phase 2φ+const. Then the process repeats, and the phase which is transformed at each next modulation period evolves according to the double expanding circle map. In the presence of compression along other (transverse) directions, this corresponds to the attractor that is the Smale – Williams solenoid embedded in the infinite-dimensional phase space of the time-delay system.

Figure 5 shows the waveform of the variable x, which corresponds to the described regime. The time dynamics manifests a sequence of bursts that alternate with periods of activity suppression. Bursts follow with the period of modulation of parameters, and the phases of oscillations (spikes) from one stage of activity to the other vary chaotically, in accordance with the Bernoulli map. Since the parameters $a_{0,1}$, $b_{0,1}$, c, ε, Ω are chosen numerically the same as for the illustrative calculations in the previous section, the waveform is very similar to those in graphs for subsystems of the finite-dimensional model in Fig. 1.

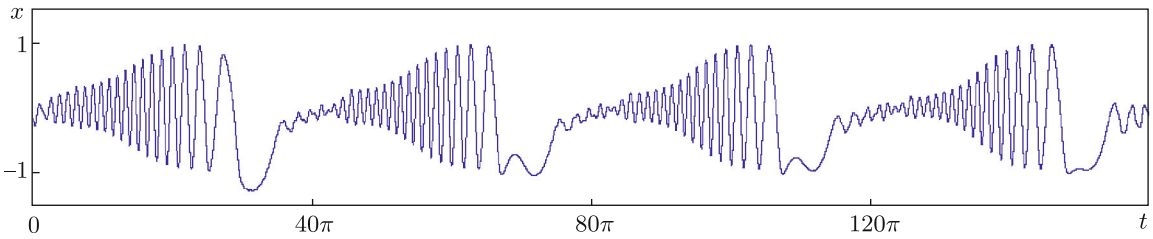

Fig. 5. Waveform of the dynamical variable $x(t)$ on four periods of parameter modulation for the system with time-delay (3.1). The values of the parameters are $a_0 = a_1 = 1.5$, $b_0 = b_1 = 0.1$, $c_0 = 0.2$, $\varepsilon = 0.3$, $\Omega = 0.05$.

In Fig. 6a a portrait of an attractor for the stroboscopic map is shown. This is a two-dimensional projection of the Smale – Williams solenoid from the infinite-dimensional phase space of the system. It has a fractal transverse structure of filaments, which can be seen on the inset showing this structure with magnification. The diagram in Fig. 6b, obtained from the numerical integration of Eq. (2.2) over a large number of modulation periods, illustrates the transformation of the oscillation phases in successive stages of activity in accordance with the double expanding circle map. The picture of the attractor projection and the diagram for the angular variable demonstrate an obvious similarity with the graphs for the finite-dimensional model in Fig. 2.

For a system with delay, the total number of Lyapunov exponents is infinite. We can find the first few exponents, performing simultaneously a numerical solution of Eq. (3.1) together with the appropriate number of variational equations and with Gram – Schmidt orthogonalization of the perturbation vectors in the framework of the traditional Benettin method adapted for time-delay systems [24, 32]. The Lyapunov exponents calculated for the attractor shown in Fig. 5 are the following:

$$\Lambda = \{0.677,\ -0.920,\ -2.39,\ -2.91,\ -3.25,\ -3.40,\ -3.63\ \ldots\}, \tag{3.3}$$

and the dimension of the attractor in the stroboscopic section according to the Kaplan – Yorke formula is $D_{KY} = 1 + \Lambda_1/|\Lambda_2| \approx 1.74$.

Figure 7 shows three largest Lyapunov exponents of the stroboscopic map of the system with time-delay versus the parameter c with other parameters constant. The range of the parameter where the largest Lyapunov exponent is close to the constant value $\ln 2$, corresponds to the region of the Smale – Williams attractor, where structurally stable hyperbolic chaos takes place. In the right part of the graph, we can see both regimes corresponding to nonhyperbolic chaos with a positive exponent, and the dips in the graph corresponding to the periodicity windows.

Figure 8 shows a chart of regimes for the time-delay system in the parameter plane, where the regions indicated by certain colors are identified using the Lyapunov exponents as described in

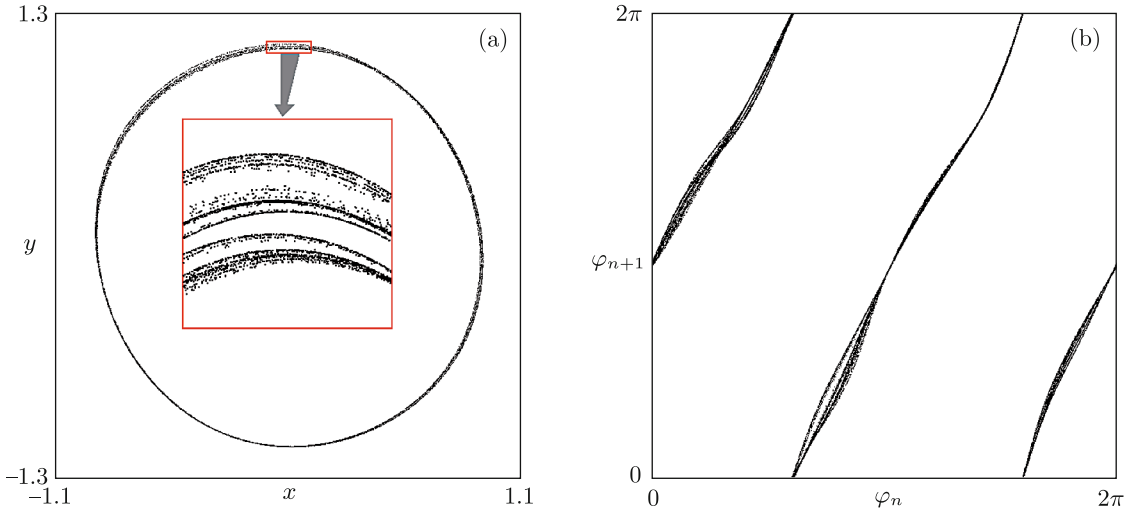

Fig. 6. Two-dimensional projection of the Smale – Williams attractor for the Poincaré map of the time-delay system (3.1) with the transverse structure of the filaments shown on the inset with magnification (a), and the diagram of phases for the spike oscillations at successive bursts, illustrating the doubling of the angular variable in each period of modulation (b). The system parameters are $a_0 = a_1 = 1.5$, $b_0 = b_1 = 0.1$, $c_0 = 0.2$, $\varepsilon = 0.3$, $\Omega = 0.05$.

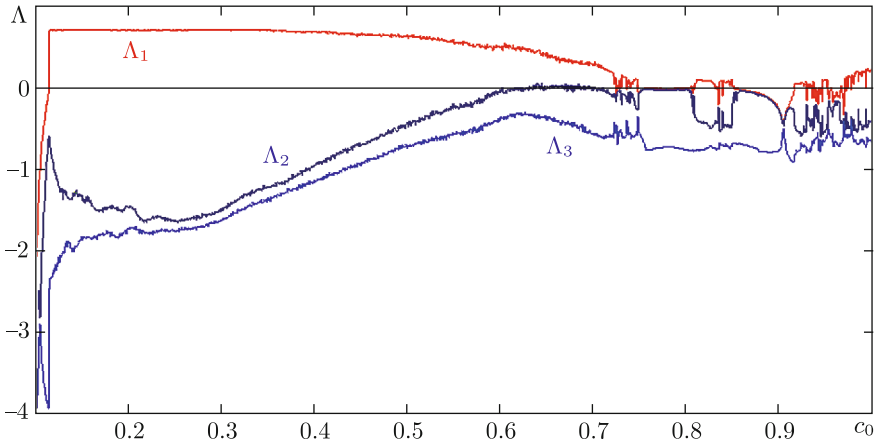

Fig. 7. Three largest Lyapunov exponents of the map (3.2) for the time-delay system with $\Omega = 0.05$, $\tau = 20\pi$, $\varepsilon = 0.5$, $a_0 = a_1 = 1.5$, $b_0 = b_1 = 0.1$.

the previous section. We can see areas corresponding to the attractor in the form of the Smale – Williams solenoid SW, areas of periodic and quasi-periodic dynamics, respectively, P and Q, and also domains of nonhyperbolic chaos, denoted by black color, where the largest Lyapunov exponent is positive, while the sum of the first two exponents is negative. In addition, a green-colored region of chaotic dynamics, where the sum of the first two exponents is positive, and the blue region of hyperchaos characterized by two positive Lyapunov exponents are shown in the chart. (The last two types of dynamics were absent in the chart for the finite-dimensional system of Fig. 4.) At the top part of the chart we can see formations similar to those observed in the same region of parameters for the finite-dimensional system, namely, the regions of quasi-periodic dynamics Q and the periodic behavior P, and also the region of nonhyperbolic chaos with inclusions of areas corresponding to the periodicity windows.

The shape and location of the SW regions, where the Smale – Williams hyperbolic chaotic attractors are realized, look similar in both charts of Fig. 8 and Fig. 4. Differences are found as we consider scenarios of exit from these areas under variation of the parameters.

When moving along the parameters plane of the time-delay system from the bottom to the top, the destruction of hyperbolic chaos is accompanied, as can be concluded, by involvement of

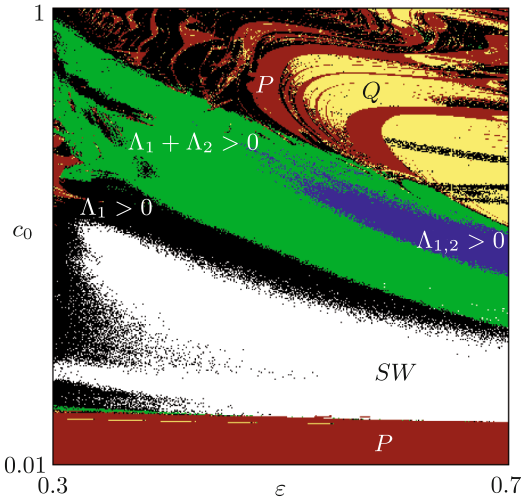

Fig. 8. Parameter plane chart for the system (3.1), where the regions indicated by a certain color and the corresponding legends, are identified by analysis of the Lyapunov exponents. Other parameters are: $\Omega = 0.05$, $a_0 = a_1 = 1.5$, $b_0 = b_1 = 0.1$, $\tau = 20\pi$.

additional directions in the phase space in the dynamics. This is evidenced by the presence of a region where $\Lambda_1 + \Lambda_2 > 0$. The attractor, even being localized inside the absorbing domain of toroidal form in the phase space, cannot be a classical Smale – Williams solenoid. Indeed, in this case, in the transverse direction not compression, but expansion of elements of two-dimensional tangent subspace takes place, and this makes it impossible to form a transverse Cantor-like structure typical of the solenoids in the form of filaments. The dimension of the attractor estimated by the Kaplan – Yorke formula (2.7) in this region is $D_{KY} > 2$, while for the Smale – Williams solenoid it should be in the interval $1 < D_{KY} < 2$.

In contrast to the finite-dimensional system, where the destruction of hyperbolicity is associated with deformation of the graph of the iterative diagram, which consists of relatively distinct branches, in this case the broadening of the branches is observed, transforming into some transversally widened formations.

4. NUMERICAL TEST OF HYPERBOLICITY OF ATTRACTORS FOR THE TIME-DELAY SYSTEM

The method for verifying hyperbolicity of attractors originally proposed in [33, 34] is that, for a typical trajectory on an attractor, the variational equations for the perturbation vectors are first solved in direct time to determine the unstable subspace, and then in the reverse time to determine the stable subspace. Further, for a set of points on the trajectory, the angles between these subspaces are calculated, and the character of the angular distribution is analyzed. If it is separated from the region of zero angles, then it indicates the hyperbolic nature of the attractor, whereas the appearance of the angles close to zero indicates that there is no hyperbolicity. For a system of two alternately excited FitzNew – Nagumo oscillators, this method was applied in [13, 14] and showed its effectiveness for recognizing the hyperbolic and nonhyperbolic chaos.

In the case of systems with time-delay, the problem is that the dimension of the phase space and, accordingly, the dimension of the contracting subspace is infinite. This problem can be overcome using a version of the method, where identification of the contracting subspace is based not on using vectors belonging to it, but by means of vectors relating to its orthogonal complement, whose dimension is usually small [35, 36]. These vectors are obtained from the adjoint set of linearized equations, the method of constructing of which for systems with one or several delay times is elaborated in [36, 37].

For our system

$$\begin{aligned} \dot{x} &= c_0 x - \frac{1}{3}x^3 - y, \\ \dot{y} &= a(t)x - b(t)y + \varepsilon \dot{x}^2(t-\tau), \\ a(t) &= a_0 - a_1 \sin \Omega t, \quad b(t) = b_0 - b_1 \cos \Omega t, \end{aligned} \tag{4.1}$$

the variational equations near the reference phase trajectory have the form

$$\begin{aligned}\dot{\tilde{x}} &= c_0\tilde{x} - x^2\tilde{x} - \tilde{y},\\ \dot{\tilde{y}} &= a(t)\tilde{x} - b(t)\tilde{y} + 2\varepsilon\dot{x}(t-\tau)\dot{\tilde{x}}(t-\tau).\end{aligned} \tag{4.2}$$

The adjoint system is derived in the manner described in [36, 37] as a system of equations with a deviating argument of the advanced type

$$\begin{aligned}\dot{\xi} &= -(c_0 - x^2)\xi - a(t)\eta - 2\varepsilon(c_0 - x^2)\Big(c_0x - \frac{1}{3}x^3 - y\Big)\eta(t+\tau),\\ \dot{\eta} &= \xi + b(t)\eta + 2\,\varepsilon\Big(c_0x - \frac{1}{3}x^3 - y\Big)\eta(t+\tau).\end{aligned} \tag{4.3}$$

The equations are constructed so that, for the vectors given by Eqs. (4.2) and (4.3), the inner product defined by the relation

$$\mathbf{x}\cdot\xi = \tilde{x}(t)\xi(t) + \tilde{y}(t)\eta(t) - 2\varepsilon\int\limits_{t-\tau}^{t}\dot{x}(\theta)\dot{\tilde{x}}(\theta)\eta(\tau+\theta)d\theta \tag{4.4}$$

remains constant in time in the course of dynamical evolution.

In the parameter region SW in Fig. 6 interesting for us, the unstable subspace of trajectories belonging to the attractor is one-dimensional, and the same is true for the orthogonal complement to the stable subspace. The procedure consists in the following: first, a long segment of the time dependences $x(t)$, $y(t)$ corresponding to a reference trajectory of the system (4.1) is calculated with simultaneous integration of the variation equations (4.2), which produce a solution that corresponds to a perturbation vector with a positive Lyapunov exponent along the reference trajectory. Further, in the reverse time along the same trajectory, the adjoint system is integrated. Although in its formal notation (4.3) it is of advanced type, in the reverse time the solutions behave as for customary retarding-time equations, so that there are no troubles associated with the mathematical nature of the equations. At the end of the procedure, the angles are calculated through the inner product of pairs of vectors related to identical points of the base trajectory at different moments of time, and a histogram of their distribution is presented graphically.

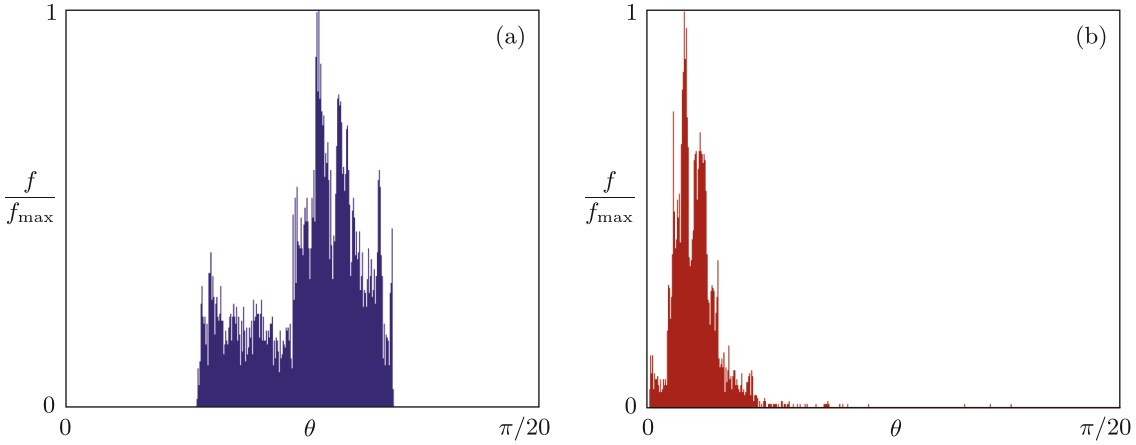

Fig. 9. Histograms of the intersection angles of stable and unstable subspaces for a hyperbolic attractor at $\varepsilon = 0.5$, $c_0 = 0.2$ (a) and a nonhyperbolic attractor at $\varepsilon = 0.4$, $c_0 = 0.55$ in the system (4.1). Other parameters are: $\Omega = 0.05$, $\tau = 20\pi$, $a_0 = a_1 = 1.5$, $b_0 = b_1 = 0.1$.

Figure 9a shows a histogram of the intersection angles for the stable and unstable subspaces for a trajectory on the attractor representing the Smale – Williams solenoid at $c_0 = 0.2$, $\varepsilon = 0.5$, and other parameters are indicated in the caption. The attractor has the Lyapunov exponents

$$\Lambda = \{0.68,\ -1.47,\ -1.71,\ -1.90,\ -2.10,\ \ldots\},$$

and its Kaplan – Yorke dimension is $D_{KY} = 1 + \Lambda_1/|\Lambda_2| \approx 1.46$. For comparison, Fig. 9b shows a histogram for the attractor at $c_0 = 0.55$, $\varepsilon = 0.4$, which is not hyperbolic. Its Lyapunov exponents are

$$\Lambda = \{0.56,\ -0.66,\ -0.95,\ -1.27,\ -1.51,\ \ldots\},$$

and the Kaplan – Yorke dimension is $D_{KY} = 1 + \Lambda_1/|\Lambda_2| \approx 1.85$.

The fact that the distribution in Fig. 9a is separated from zero, confirms the hyperbolic nature of the attractor of the Poincaré map. Similar results are obtained with variation of the system parameters in a rather wide range (*SW* region in Fig. 6), which corresponds to the inherent roughness (structural stability) of the hyperbolic attractor.

5. CONCLUSION

In the present paper we demonstrate the occurrence of the rough hyperbolic chaos associated with the Smale – Williams attractor in systems based on coupled neurons and delayed-feedback neurons with alternating excitation and suppression of activity due to periodic modulation of parameters. These results may be interesting both from the point of view of phenomenology in the context of neurodynamics and within the framework of constructing technical systems, for example, electronic noise generators, insensitive to variation of parameters, interferences and noise.

For a system of two alternately excited neurons, in the parameter plane a chart of regimes is presented containing a wide region of hyperbolic chaos, and scenarios of its destruction at the exit from this region are discussed.

A new model able to demonstrate hyperbolic chaos is introduced in the form of a single FitzHugh – Nagumo neuron with parameter modulation supplemented with delayed feedback loop, where the quadratic transformation of the transmitted signal is provided. Numerical results confirm the hyperbolic nature of chaos in a wide range of parameters for the system with delay.

It can be assumed that interesting examples of complex dynamics, including structurally stable chaos and hyperchaos, may be realized in many other systems composed as chains and networks based on model neurons. An interesting question is a possible significance of these phenomena for functioning of natural neural networks and for their technical analogs.

In any case, the results obtained make it possible to implement electronic generators of robust chaos on the basis of systems of coupled elements in the form of the Bonhoeffer – van der Pol oscillators equivalent in their dynamics to the model FitzHugh – Nagumo neurons. The structurally stable systems for various plausible chaos applications (schemes of hidden communication [38, 39], noise radar [40], cryptographic applications [41, 42], generation of random numbers [43, 44]) are preferable because of insensitivity of characteristics of generated chaos to interferences, noises, manufacturing imperfections, etc.

ACKNOWLEDGMENTS

This work was supported by the Russian Science Foundation (grant No 17-12-01008). The authors thank I. R. Sataev for a useful discussion.

REFERENCES

1. FitzHugh, R., Impulses and Physiological States in Theoretical Models of Nerve Membrane, *Biophys. J.,* 1961, vol. 1, no. 6, pp. 445–466.
2. Nagumo, J., Arimoto, S., and Yoshizawa, S., An Active Pulse Transmission Line Simulating Nerve Axon, *Proc. of the IRE,* 1962, vol. 50, no. 10, pp. 2061–2070.
3. Andronov, A. A., Vitt, A. A., and Khaikin, S. E., *Theory of Oscillators,* Oxford: Pergamon, 1966.
4. Gaponov-Grekhov, A. V. and Rabinovich, M. I., L. I. Mandel'shtam and the Modern Theory of Nonlinear Oscillations and Waves, *Physics–Uspekhi,* 1979, vol. 22, no. 8, pp. 590–614; see also: *Uspekhi Fiz. Nauk,* 1979, vol. 128, no. 8, pp. 579–624.
5. Rabinovich, M. I. and Trubetskov, D. I., *Oscillations and Waves in Linear and Nonlinear Systems,* Dordrecht: Kluver, 1989.
6. Landa, P. S., *Nonlinear Oscillations and Waves in Dynamical Systems,* Math. Appl., vol. 360, Dordrecht: Springer, 2013.
7. Smale, S., Differentiable Dynamical Systems, *Bull. Amer. Math. Soc.,* 1967, vol. 73, no. 6, pp. 747–817.

8. *Dynamical Systems 9: Dynamical Systems with Hyperbolic Behaviour,* D. V. Anosov (Ed.), Encyclopaedia Math. Sci., vol. 66, Berlin: Springer, 1995.
9. Shilnikov, L., Mathematical Problems of Nonlinear Dynamics: A Tutorial, *Internat. J. Bifur. Chaos Appl. Sci. Engrg.,* 1997, vol. 7, no. 9, pp. 1953–2001.
10. Andronov, A. and Pontryagin, L., Systèmes grossiers, *Dokl. Akad. Nauk. SSSR,* 1937, vol. 14, no. 5, pp. 247–250 (Russian).
11. Kuznetsov, S. P., Dynamical Chaos and Uniformly Hyperbolic Attractors: From Mathematics to Physics, *Phys. Uspekhi,* 2011, vol. 54, no. 2, pp. 119–144; see also: *Uspekhi Fiz. Nauk,* 2011, vol. 181, no. 2, pp. 121–149.
12. Kuznetsov, S. P., *Hyperbolic Chaos: A Physicist's View,* Berlin: Springer, 2012.
13. Jalnine, A. Yu., Hyperbolic and Non-Hyperbolic Chaos in a Pair of Coupled Alternately Excited FitzHugh – Nagumo Systems, *Commun. Nonlinear Sci. Numer. Simul.,* 2015, vol. 23, nos. 1–3, pp. 202–208.
14. Jalnine, A. Yu., From Quasiharmonic Oscillations to Neural Spikes and Bursts: A Variety of Hyperbolic Chaotic Regimes Based on Smale – Williams Attractor, *Rus. J. Nonlin. Dyn.,* 2016, vol. 12, pp. 53–73 (Russian).
15. Kuznetsov, S. P. and Ponomarenko, V. I., Realization of a Strange Attractor of the Smale – Williams Type in a Radiotechnical Delay-Feedback Oscillator, *Tech. Phys. Lett.,* 2008, vol. 34, no. 9, pp. 771–773; see also: *Pisma Zh. Tekh. Fiz.,* 2008, vol. 34, no. 18, pp. 1–8.
16. Kuznetsov, S. P. and Pikovsky, A. S., Hyperbolic Chaos in the Phase Dynamics of a Q-Switched Oscillator with Delayed Nonlinear Feedbacks, *Europhys. Lett.,* 2008, vol. 84, no. 1, 10013, 5 pp.
17. Baranov, S. V., Kuznetsov, S. P., and Ponomarenko, V. I., Chaos in the Phase Dynamics of Q-Switched van der Pol Oscillator with Additional Delayed Feedback Loop, *Izvestiya VUZ, Applied Nonlinear Dynamics,* 2010, vol. 18, no. 1, pp. 11–23 (Russian).
18. Kuznetsov, A. S. and Kuznetsov, S. P., Parametric Generation of Robust Chaos with Time-Delayed Feedback and Modulated Pump Source, *Commun. Nonlinear Sci. Numer. Simul.,* 2013, vol. 18, no. 3, pp. 728–734.
19. Arzhanukhina, D. S. and Kuznetsov, S. P., Robust Chaos in Autonomous Time-Delay System, *Izvestiya VUZ, Applied Nonlinear Dynamics,* 2014, vol. 22, no. 2, pp. 36–49 (Russian).
20. Kuznetsov, S. P. and Pikovsky, A., Attractor of Smale – Williams Type in an Autonomous Time-Delay System, arXiv:1011.5972 (2010).
21. Moon, F. C. and Holmes, W. T., Double Poincaré Sections of a Quasi-Periodically Forced, Chaotic Attractor, *Phys. Lett. A,* 1985, vol. 111, no. 4, pp. 157–160.
22. Kuznetsov, A. P., Kuznetsov, S. P., Pikovsky, A. S., and Turukina, L. V., Chaotic Dynamics in the Systems of Coupling Nonautonomous Oscillators with Resonance and Nonresonance Communicator of the Signal, *Izvestiya VUZ, Applied Nonlinear Dynamics,* 2007, vol. 15, no. 6, pp. 75–85 (Russian).
23. Kaplan, J. L. and Yorke, J. A., A Chaotic Behavior of Multi-Dimensional Differential Equations, in *Functional Differential Equations and Approximations of Fixed Points,* H.-O. Peitgen, H.-O. Walther (Eds.), Lecture Notes in Math., vol. 730, Berlin: Springer, 1979, pp. 204–227.
24. Farmer, J. D., Chaotic Attractors of an Infinite-Dimensional Dynamical System, *Phys. D,* 1981/82, vol. 4, no. 3, pp. 366–393.
25. Kuznetsov, S. P., *Dynamical Chaos,* 2nd ed., Moscow: Fizmatlit, 2006 (Russian).
26. Isaeva, O. B., Kuznetsov, S. P., Sataev, I. R., Savin, D. V., and Seleznev, E. P., Hyperbolic Chaos and Other Phenomena of Complex Dynamics Depending on Parameters in a Nonautonomous System of Two Alternately Activated Oscillators, *Internat. J. Bifur. Chaos Appl. Sci. Engrg.,* 2015, vol. 25, no. 12, 1530033, 15 pp.
27. Glass, L., Guevara, M. R., Shrier, A., and Perez, R., Bifurcation and Chaos in a Periodically Stimulated Cardiac Oscillator, *Phys. D,* 1983, vol. 7, nos. 1–3, pp. 89–101.
28. Argyris, J. H., Faust, G., Haase, M., and Friedrich, R., *An Exploration of Dynamical Systems and Chaos: Completely Revised and Enlarged Second Edition,* Berlin: Springer, 2015.
29. Gallas, J. A. C., Dissecting Shrimps: Results for Some One-Dimensional Physical Models, *Phys. A,* 1994, vol. 202, nos. 1–2, pp. 196–223.
30. Bellman, R. E. and Cooke, K. L., *Differential-Difference Equations,* New York: Acad. Press, 2012.
31. El'sgol'ts, L. E. and Norkin, S. B., *Introduction to the Theory and Application of Differential Equations with Deviating Arguments,* New York: Acad. Press, 2012.
32. Balyakin, A. A. and Ryskin, N. M., Peculiarities of Calculation of the Lyapunov Exponents Set in Distributed Self-Oscillated Systems with Delayed Feedback, *Izvestiya VUZ, Applied Nonlinear Dynamics,* 2007, vol. 15, no. 6, pp. 3–21 (Russian).
33. Lai, Y.-Ch., Grebogi, C., Yorke, J. A., and Kan, I., How Often Are Chaotic Saddles Nonhyperbolic?, *Nonlinearity,* 1993, vol. 6, no. 5, pp. 779–797.
34. Anishchenko, V. S., Kopeikin, A. S., Kurths, J., Vadivasova, T. E., Strelkova, G. I., Studying Hyperbolicity in Chaotic Systems, *Phys. Lett. A,* 2000, vol. 270, no. 6, pp. 301–307.

35. Kuptsov, P. V., Fast Numerical Test of Hyperbolic Chaos, *Phys. Rev. E,* 2012, vol. 85, no. 1, 015203, 4 pp.
36. Kuptsov, P. V. and Kuznetsov, S. P., Numerical Test for Hyperbolicity of Chaotic Dynamics in Time-Delay Systems, *Phys. Rev. E,* 2016, vol. 94, no. 1, 010201(R), 7 pp.
37. Kuptsov, P. V. and Kuznetsov, S. P., Numerical Test for Hyperbolicity in Chaotic Systems with Multiple Time Delays, *Commun. Nonlinear Sci. Numer. Simul.,* 2018, vol. 56, pp. 227–239.
38. Dmitriev, A. S., Efremova, E. V., Maksimov, N. A., and Panas, A. I., *Generation of Chaos*, Moscow: Tekhnosfera, 2012 (Russian).
39. Koronovskii, A. A., Moskalenko, O. I., and Hramov, A. E., On the Use of Chaotic Synchronization for Secure Communication, *Physics–Uspekhi,* 2009, vol. 52, no. 12, pp. 1213–1238; see also: *Uspekhi Fiz. Nauk,* 2009, vol. 179, no. 12, pp. 1281–1310.
40. Lukin, K. A., Noise Radar Technology, *Telecommunications and Radio Engineering,* 2001, vol. 55, no. 12, pp. 8–16.
41. Baptista, M. S., Cryptography with Chaos, *Phys. Lett. A,* 1998, vol. 240, nos. 1–2, pp. 50–54.
42. *Chaos-Based Cryptography: Theory, Algorithms and Applications,* L. Kocarev, Sh. Lian (Eds.), Studies in Computational Intelligence, vol. 354, Berlin: Springer, 2011.
43. Stojanovski, T. and Kocarev, L., Chaos-Based Random Number Generators: 1. Analysis, *IEEE Trans. Circuits Systems 1 Fund. Theory Appl.,* 2001, vol. 48, no. 3, pp. 281–288.
44. Stojanovski, T. and Kocarev, L., Chaos-Based Random Number Generators: 2. Practical Realization, *IEEE Trans. Circuits Systems 1 Fund. Theory Appl.,* 2001, vol. 48, no. 3, pp. 382–385.